The Intact Human Acetylcholinesterase C-Terminal Oligomerization Domain Is α-Helical *in Situ* and in Isolation, but a Shorter Fragment Forms β-Sheet-Rich Amyloid Fibrils and Protofibrillar Oligomers†

Matthew G. Cottingham,‡ Jan L. A. Voskuil,§,|| and David J. T. Vaux*,‡

Sir William Dunn School of Pathology, University of Oxford, Oxford OX1 3RE, U.K., and Synaptica Ltd., 551 Harwell International Business Centre, Didcot OX11 0QJ, U.K.

Received May 12, 2003; Revised Manuscript Received July 11, 2003

ABSTRACT: A 14-residue fragment of the C-terminal oligomerization domain, or T-peptide, of human acetylcholinesterase (AChE) shares sequence homology with the amyloid-β peptide implicated in Alzheimer's disease and can spontaneously self-assemble into classical amyloid fibrils under physiological conditions [Greenfield, S. A., and Vaux, D. J. (2002) *Neuroscience 113*, 485−492; Cottingham, M. G., Hollinshead, M. S., and Vaux, D. J. (2002) *Biochemistry 41*, 13539−13547]. Here we demonstrate that the conformation of this $AChE_{586-599}$ peptide, both before and after fibril formation, is different from that of a longer peptide, T_{40}, corresponding to the entire 40-amino acid T-peptide (residues 575−614 of AChE). This peptide is prone to homomeric hydrophobic interactions, consistent with its role in AChE subunit assembly, and possesses an α-helical structure which protects against the development of the β-sheet-rich amyloidogenic conformation favored by the shorter constituent $AChE_{586-599}$ fragment. Using a conformation-sensitive monoclonal antibody raised against the α-helical T_{40} peptide, we demonstrate that the conformation of the T-peptide domain within intact AChE is antigenically indistinguishable from that of the synthetic T_{40} peptide. A second monoclonal antibody raised against the fibrillogenic $AChE_{586-599}$ fragment recognizes not only β-sheet amyloid aggregates but also SDS-resistant protofibrillar oligomers. A single-antibody sandwich ELISA confirms that such oligomers exist at micromolar peptide concentrations, well below that required for formation of classical amyloid fibrils. Epitope mapping with this monoclonal antibody identifies a region near the N-terminus of the peptide that remains accessible in oligomer and fibril alike, suggesting a model for the arrangement of subunits within $AChE_{586-599}$ protofibrils and fibrils.

The well-known classical function of the enzyme acetylcholinesterase (AChE, EC 3.1.1.8) is to hydrolyze the neurotransmitter acetylcholine at mammalian neuromuscular junctions and synapses in the central nervous system (*3*). AChE exists in a plurality of molecular isoforms governed by alternative splicing events and interactions with other gene products (*4*). T-Form, or synaptic, AChE is the splice variant expressed in the mammalian brain and muscles, and it posesses a 40-residue C-terminal tail domain, encoded by the alternatively spliced exon 6. This domain, the T-peptide, is the key to higher-order subunit association, and is crucial in determining the functional localization of synaptic AChE (*5*). It permits the assembly of the enzyme into soluble homomeric tetramers (G_4) which together with T-form dimers (G_2) and monomers (G_1) account for a small proportion (<10%) of AChE in the mammalian brain. The T-peptide also governs the interaction of AChE with a proline-rich attachment domain (PRAD) present in PRiMA, the proline-rich membrane anchor, expressed on neuronal membranes; and ColQ, a collagen triple helix anchored to the basal lamina in neuromuscular junctions (*6*, *7*).

The crystal structure of the catalytic domain of AChE was determined as early as 1991 (*8*), but the organization of the subunits in tetrameric AChE and the positioning and structure of the T-peptides in homomeric and heteromeric isoforms remain unclear, mainly since the vast majority of crystals have been grown from truncated enzymes lacking the C-terminal domain. Three crystal structures of tetrameric AChE have been reported (*9*, *10*), each with a different arrangement of subunits, and all lacking information about the structure or position of the T-peptides. However, it has been possible to make a number of inferences about the structure of the cholinesterase T-peptide. It possesses a series of highly conserved aromatic residues which are critical both for assembly of disulfide-linked dimers into homomeric tetramers (*11*) and for attachment of tetramers to PRAD (*12*). The hydrophobic residues are thought to lie along one face of a predicted amphiphilic α-helix formed by the T-peptide (*13*), providing a hydrophobic driving force for the assembly of dimers into tetramers, just as the amphiphilic $\alpha_{7,8}$ and α_{10} helices of the catalytic domain provide the hydrophobic driving force for assembly of monomers into dimers (*14*,

† This work was supported by a research grant from Synaptica Ltd., a spin-out company from the University of Oxford.

* To whom correspondence should be addressed. E-mail: vaux@molbiol.ox.ac.uk. Telephone: +44 (1865)275544. Fax: +44 (1865)-275501.

‡ University of Oxford.

§ Synaptica Ltd.

|| Current address: Sir William Dunn School of Pathology, University of Oxford, Oxford OX1 3RE, U.K.

10.1021/bi034768i CCC: $25.00
Published on Web 08/22/2003

Table 1: Synthetic Peptides[a]

T_{40} (=$AChE_{575-614}$)	DTLDEAERQWK**AEF**HRWSSYMV**H**WKNQFDHYSKQDR<u>S</u>SDL
$AChE_{586-599}$	**AEF**HRWSSYMV**H**WK
$BuChE_{573-586}$	**AGF**HRWNNYMMDWK
$Aß_{1-16}$	DA**EF**RHDSGYEV**H**HQK
$Aß_{1-42}$	DA**EF**RHDSGYEV**H**HQKLVFFAEDVGSNKGAIIGLMVGGVVIA
$Aß_{25-35}$	GSNKGAIIGLM

[a] Alignment of synthetic peptides from acetylcholinesterase (AChE) and butyrylcholinesterase (BuChE) at the region sharing sequence similarity (*1*, *2*) with the Alzheimer's disease β-amyloid peptide (Aβ). Identical residues shared by Aβ and AChE or BuChE are shown in bold. T_{40} corresponds to the entire T-peptide (or the C-terminal oligomerization domain, encoded by the alternatively spliced exon 6) of AChE, running from residue 575 to 614. In this paper, T_{40} refers to the synthetic peptide and T-peptide to the same sequence present as a domain of AChE, though it should be noted that there is a cysteine at position 611 of AChE (corresponding to residue 37 of T_{40}) which is mutated to a serine in the synthetic peptide (underlined) to prevent intermolecular disulfide bond formation. The AChE and BuChE residue numberings refer to the human sequence including the N-terminal signal peptides (31 residues in the case of AChE and 28 in that of BuChE). An additional peptide, scrambled $AChE_{586-599}$, with the sequence HSWRAEVFHKYWSM is used as a control.

15). This interpretation can explain why G_1 and G_2 T-form AChE are amphiphilic, since the T-peptides are exposed, but homomeric G_4 is not, since the T-peptides are in association with one another and are not therefore exposed to solvent (*16*). We report that T_{40}, a 40-amino acid synthetic peptide corresponding to the C-terminal T-peptide domain of AChE, possesses an α-helical structure in solution. This observation corroborates a recently determined crystal structure of synthetic T_{40} complexed with a synthetic PRAD peptide, reported in posters presented at two recent conferences (*17*, *18*). Furthermore, we use a conformation-dependent monoclonal antibody, 55C, which binds selectively to this α-helical structure, to immunoprecipitate intact AChE, providing, to our knowledge, the first evidence for an *in situ* α-helical conformation of the T-peptide domain.

The current work also concerns the adoption of an alternative, non-native conformation by a stretch of the T-peptide whose sequence is similar to that of Aβ (*1*, *2*), the 40−42-amino acid fragment of the Alzheimer precursor protein (APP) (*19*, *20*), which is the focus of the current understanding of the etiology of the disease (*21*). The homologous region lies near the N-terminus of Aβ, but near the middle of the AChE T-peptide, which runs from position 575 to the end of the sequence at position 614[1] (see Table 1). We have previously reported that a synthetic peptide, $AChE_{586-599}$, designed to encompass the region of sequence similarity within a hypothetical tryptic fragment, is capable of forming amyloid fibrils under physiological conditions. Just like those formed *in vitro* by Aβ, these fibrous $AChE_{586-599}$ aggregates possess all the classical hallmarks of amyloid fibrils (*22*), and are neurotoxic *in vitro* (*2*).

Using a second conformation-specific monoclonal antibody, 105A, we report here that $AChE_{586-599}$ forms protofibrillar oligomers that can be detected in two different experimental systems. This observation further confirms the identification of $AChE_{586-599}$ as a typical amyloidogenic peptide, since soluble, diffusible, oligomeric protofibrils, rather than large fibrillar aggregates, are currently thought to be responsible for the toxicity of Aβ (*23*−*30*) and of other amyloidogenic polypeptides (*31*). The monoclonal antibody 105A is also used to produce a model of the subunit organization in $AChE_{586-599}$ amyloid assemblies, by mapping its epitope to a region near the N-terminus of the peptide.

It is well-known that a range of polypeptides, with widely varying lengths and sequences, are able to form amyloid fibrils associated with a number of slow-onset degenerative diseases (*32*, *33*). The ability to adopt the generic crossed β-sheet amyloid structure (*34*) may be a common property of all polypeptide chains (*35*, *36*), since a number of proteins not known to be associated with any disease can be induced to form cytotoxic amyloid fibrils in the laboratory by aggressive chemical destabilization of the native polypeptide fold (*37*−*42*). The crucial dependence of fibrillogenesis under physiological conditions upon sequence is here exemplified by the absence of detectable fibril or protofibril formation by $BuChE_{573-586}$, a synthetic peptide derived from the cognate region of the closely related enzyme butyrylcholinesterase (BuChE).

The identification of a fibrillogenic region of AChE may be relevant to the pathophysiology of Alzheimer's disease, since the cholinergic system, and more specifically AChE, is heavily implicated, in four principal ways, in the disease process. First, the loss of cholinergic neurons is one of the earliest and most pronounced neuropathological changes (*43*−*45*), and there is a good though not perfect correlation between regions of the brain rich in AChE and regions prone to degeneration in Alzheimer's disease (*46*, *47*). Second, biochemical studies of affected areas of the Alzheimer brain (*44*, *48*−*50*) have revealed not only a huge decrease (up to 90%) in the amount of PRiMA-associated membrane-bound G_4 AChE in the Alzheimer brain (attributable to the degeneration of cholinergic neurons) but also a marked increase in the levels of the less abundant amphiphilic G_1 and G_2 species, probably due to *de novo* production (*51*). Third, AChE is aberrantly localized within Alzheimer's disease senile plaques (*52*−*54*), from a very early stage in their development (*55*, *56*). Finally, it has recently been reported by Inestrosa and co-workers that AChE is able to interact with Aβ *in vitro* and to increase the rate and extent of assembly of Aβ into fibrillar complexes containing the enzyme (57−*60*).

In this paper, we use spectroscopic methods and new conformation-specific monoclonal antibodies to demonstrate that, consistent with the current understanding, the C-terminal T-peptide domain of the enzyme AChE has a stable native α-helical structure. Nevertheless, we also show that part of this domain is capable, when in isolation, of adopting a different structure, and of forming cytotoxic amyloid fibrils and protofibrils. It remains to be established whether such an altered conformation can occur *in vivo*, where it might account for the association of AChE with Aβ in senile plaques.

EXPERIMENTAL PROCEDURES

Synthetic Peptides. The peptides T_{40}, $AChE_{586-599}$, eight-branch multiantennary $AChE_{586-599}$ (MAP-$AChE_{586-599}$),

[1] The human residue numbering including the signal peptide is used throughout.

scrambled $AChE_{586-599}$, $BuChE_{573-586}$, $A\beta_{1-16}$, and $A\beta_{25-35}$ were synthesized using the standard Fmoc methodology and purified to >95% using HPLC by M. Pitkeathley at the Oxford Centre for Molecular Science (University of Oxford). See Table 1 for the sequences of the peptides. $A\beta_{1-42}$ was purchased from Oncogene Research Products. The peptides were divided into small aliquots for relyophilization, and aliquots stored at −20 °C were freshly dissolved to 2 mg/mL in sterile ultrapure water before being used. The cysteine at position 611 of AChE (corresponding to position 37 of T_{40}) was mutated to a serine in the synthetic peptide to prevent intermolecular disulfide bond formation.

A panel of synthetic peptide variations on the sequence of $AChE_{586-599}$ was purchased from Chiron. The variations included alanine scanning mutants, N- and C-terminal and symmetrical truncations, and transitions and replacements from the AChE to the BuChE and Aβ sequences. The peptides were supplied in crude form and therefore contain both proteinaceous and nonproteinaceous contaminants. The peptides were stored at −20 °C and dissolved in a 50:50 acetonitrile/ultrapure water mixture at 2 mg/mL.

For reproducible formation of amyloid fibrils, it was previously found to be necessary to dilute aqueous stocks of peptide with an equal volume of buffer of twice the required final concentration (*2*). This protocol was adopted throughout the current work for all peptides. $AChE_{586-599}$ does not form fibrils in unbuffered aqueous solutions, since they have a low pH (≤4 at 1 mM) due to the presence of residual trifluoroacetic acid from the peptide synthesis. Only when the pH is brought within a window near neutral pH (6.5−8.5) is amyloidogenesis favored (*2*).

Circular Dichroism (CD) Spectroscopy. Far-UV CD spectra were obtained at 25 °C using a Jasco J-720 spectropolarimeter and quartz cuvettes with a path length of 1 mm (Hellma). Peptide solutions at a concentration of 200 μM in 50 mM sodium phosphate (pH 7.0) were prepared in the assay vessel by mixing 125 μL of a 400 μM aqueous peptide solution with 125 μL of a 100 mM buffer solution, as previously described (*2*). Spectra were recorded immediately, 90 min, 3 h, and 18 h after neutralization. Background spectra recorded in the absence of peptide were subtracted from the sample spectra.

8-Anilinonaphthalenesulfonic Acid (ANS) Fluorescence. Changes in ANS fluorescence were monitored using a BMG PolarSTAR plate reader with a 390 nm short-pass excitation and a 520 nm emission filter (bandwidth of 35 nm). ANS (Sigma) was freshly prepared as a 5 mM stock solution in water, and was used at a final concentration of 50 μM. A volume of 100 μL of 0.1 M buffer containing 100 μM ANS was added to 100 μL volumes of 400 μM peptides in aqueous solution in the wells of Greiner black-walled 96-well plates. Measurements were taken every 10 min for 12 h with agitation for 10 s after each measurement. Signals in the absence of ANS were subtracted from the measurements obtained in the presence of ANS.

Production of Mouse Monoclonal Antibodies. For immunization, T_{40} and $AChE_{586-599}$ were covalently coupled to keyhole limpet hemocyanin (KLH) at the ratio of 2 mg of peptide to 1 mg of KLH in a volume of 2 mL using an *N*-ethyl-*N*′-[(dimethylamino)propyl]carbodiimide-based conjugation kit (Pierce) according to the manufacturer's instructions. The unconjugated peptide and the coupling reagents were removed by dialysis against PBS using a 3.5 kDa molecular mass cutoff membrane. $AChE_{586-599}$ was additionally synthesized as a multiantennary peptide (MAP-$AChE_{586-599}$). Specific pathogen-free Balb/c mice were bred at the Sir William Dunn School of Pathology. Groups of four mice received intraperitoneal and subcutaneous immunizations at two sites, consisting either of 125 μL of KLH-T_{40} conjugate or of 125 μL of KLH-$AChE_{586-599}$ and 500 μg of MAP-$AChE_{586-599}$, emulsified 50:50 in Freund's complete adjuvant for the first immunizations and in incomplete adjuvant for subsequent immunizations. Test bleeds were taken from the tail vein 10 days after each immunization and were analyzed by an ELISA to determine the specific titer to the peptide antigens.

After five immunizations at biweekly intervals, a selected mouse in each group was given an intrasplenic immunization of 50 μL of KLH-conjugated peptide under halothane anesthesia. Five days later, the mouse was sacrificed and the splenocytes were harvested. The splenocytes were fused in a 1:2 ratio with NS1 mouse myeloma cells using PEG 1500, and the fused cells were plated in αMEM supplemented with 20% FCS, 10% BM-Condimed H1 (Roche), nonessential amino acids, 1 mM sodium pyruvate, 2 mM glutamine, and 3.4 μL/L β-mercaptoethanol, with, for selection of hybrids, 100 μM hypoxanthine, 0.4 μM aminopterin, and 16 μM thymidine. After 5 days, the wells were fed with medium lacking selection reagents, and after 10−15 days, the supernatants were screened by an ELISA (see below). The secreting hybridomas in positive wells were subsequently cloned thrice by limiting dilution, using medium lacking BM-Condimed H1, and multiple aliquots were cryopreserved for long-term storage. This approach yielded two stable hybridoma lines, one, 55C, secreting an $IgG_1\kappa$ specifically reactive with T_{40} and the other, 105A, secreting an $IgG_1\kappa$ specifically reactive with $AChE_{586-599}$ (see Figure 2A).

Protein G Purification of Monoclonal Antibodies. For BIAcore analysis, AChE immunoprecipitation, and sandwich ELISAs, purified monoclonal antibodies were used rather than hybridoma culture supernatants. To isolate the antibodies, 100 mL of 0.2 μm-filtered hybridoma culture supernatant containing 0.1 M sodium acetate (pH 5.0) was applied to an equilibrated 2 mL protein G−Sepharose column (Pierce). The column was washed extensively with 0.1 M acetate, and the bound immunoglobulin was eluted with 0.1 M glycine (pH 2.6). Fractions of 0.9 mL were neutralized with 0.1 mL of 10× PBS, and positive fractions were pooled.

Enzyme-Linked Immunosorbent Assay (ELISA). Synthetic peptides were coated onto Costar EIA/RIA plates by drying down 1 μg of peptide per well in 50 μL of 50 mM sodium bicarbonate (pH 9.0) overnight at 37 °C. The rest of the assay was performed at room temperature. The plates were washed once in phosphate-buffered saline (pH 7.4) containing 0.05% Tween-20 (PBS-Tween) and blocked with 5 mg/mL fatty acid-free bovine serum albumin in PBS for 1 h. Subsequent incubation steps (duration of 1 h) were performed using 100 μL volumes and were separated by three washes with 250 μL of PBS-Tween per well. Antibody-containing 55C and 105A hybridoma culture supernatants were applied and incubated in a 5% CO_2 atmosphere to maintain a physiological pH. Alkaline phosphatase-conjugated goat anti-mouse IgG (Fcγ-specific, from Jackson) diluted 1:4000 in blocking buffer was used to detect bound antibody, followed

by development with 5 mg/mL *p*-nitrophenyl phosphate in a solution containing 50 mM sodium glycinate and 4 mM $MgCl_2$. The resulting absorbances were read at 405 nm. ELISAs and other microplate-based assays were always performed in duplicate, and the values that are shown are the mean absorbance of two wells, with error bars representing the standard error of the mean.

Western Blotting and Dot Blotting. For SDS−PAGE, 10 μL volumes of samples and markers (New England Biolabs) were boiled for 5 min in Laemmli's sample buffer (*61*) and loaded onto 10 to 20% or 4 to 20% precast gradient gels (Bio-Rad) which were electrophoresed at 150 V at room temperature. For nondenaturing electrophoresis, the SDS, the β-mercaptoethanol, and the boiling step were omitted from the system and 4 to 20% gradient gels (Bio-Rad) were used and run at 150 V for 4 h at 4 °C. The proteins were then electrotransferred onto nitrocellulose for 1 h at 4 °C. Dot blotting was performed by applying 2.5 μL volumes of 200 μM peptide solutions, or of a 0.1 mg/mL solution of human recombinant AChE in PBS (Sigma) directly onto nitrocellulose using a pipet. Peptide solutions were buffered in 50 mM sodium acetate (pH 4.0), sodium phosphate (pH 7.0), or sodium bicarbonate (pH 9.0). The blots were stained for 10 min with 0.1% Ponceau-S in 5% acetic acid (Sigma) to visualize bound protein, and were destained in PBS prior to blocking of the membranes with 5% nonfat milk in PBS for 1 h. Hybridoma culture supernatants were applied, and the blots were incubated for 1 h in 5% CO_2 to maintain pH, before washing with PBS containing 0.05% Tween-20. The secondary antibody, alkaline phosphatase-conjugated goat anti-mouse IgG (Fcγ-specific, from Jackson) diluted 1:4000 in blocking buffer, was applied for 1 h, and the blots were extensively washed with PBS-Tween. The bound antibody was visualized by development with Sigma BCIP/NBT substrate tablets according to the manufacturer's instructions.

Production of Recombinant Human AChE. For immunoprecipitation experiments, the source of AChE was HEK293 cells transiently transfected with recombinant human T-form (containing exon 6) *ACHE* (AChE WT) and *ACHE* truncated at the end of exon 4 (position 574 in the protein; AChE D575*) and therefore lacking the exon 6-encoded T-peptide (corresponding to the T_{40} synthetic peptide used to produce 55C), but possessing an intact catalytic domain. *ACHE* cDNA was obtained from the UK MRC HGMP Resource Centre and was cloned into the pCDNA3.1 mammalian expression vector (Invitrogen) using *Kpn*I and *Xho*I. The truncated form was generated using a mismatched PCR primer (5′-GCCTC*CTCGAG*CGTTCAGGTGGC-3′) at the 3′ end to introduce a premature stop codon (underlined) and a *Xho*I site (italic). The 5′ primer (5′-CCACAATGGC-CCCCGTACACGGC-3′) was positioned just upstream of a unique *Not*I site in *ACHE* (1640 bp from the ATG start codon), and the resulting PCR product was cloned into the full-length AChE construct in place of the wild-type sequence using *Not*I and *Xho*I. Both inserts were bidirectionally sequenced with multiple primers to confirm the correct wild-type sequence and site-specific truncation.

The plasmids were transfected into ~60% confluent HEK293 cells using polyethylenimine (*62*). Twenty-four hours after transfection, the medium (DMEM with nonessential amino acids and 10% FCS) was changed to DMEM with nonessential amino acids and 2% Ultroser (Gibco), which, unlike FCS, has low endogenous cholinesterase activity (*63*). Five to seven days later, supernatants from these cells were tested using Ellman's assay (*64*) for the presence of recombinant enzyme. The supernatants were analyzed by nondenaturing gel electrophoresis on 4 to 20% gradient gels (Bio-Rad) run overnight at 120 V and 4 °C and stained according to the method of Karnovsky and Roots (*65*) for cholinesterase activity, to verify that, as expected (*4*), the AChE (WT) enzyme existed as tetramers, dimers, and monomers but that the truncated D575* enzyme existed only as monomers retaining full enzymatic activity.

AChE Immunoprecipitation. Costar ELISA plates were coated for 2 h at room temperature with 1 μg/well of protein G-purified 105A or 55C antibody, or an unrelated isotype-matched monoclonal antibody, in 50 μL of 20 mM sodium bicarbonate (pH 9.0) per well. The plates were blocked as for an ELISA (see above), and then 100 μl of HEK293 cell culture supernatant containing AChE (WT) and AChE D575* per well, as well as supernatant from cells subjected to a mock transfection (lacking plasmid DNA), were applied to the antibody-coated plates, which were incubated in 5% CO_2 to maintain the pH. The plates were washed, and the bound AChE was detected using Ellman's assay (*64*). The reaction was allowed to continue for 2 h before the absorbances were read at 450 nm.

Surface Plasmon Resonance (BIAcore). Estimation of the binding affinity of 105A and 55C for synthetic peptides was performed using a BIAcore 2000 surface plasmon resonance instrument. The analysis was conducted at 25 °C using a flow rate of 5 μL/min with HEPES-buffered saline (HBS, pH 7.4) as the default running buffer. A carboxymethyldextran matrix CM5 sensor chip with four flow cells was activated for coupling of polypeptides via primary amines using *N*-hydrosuccinimide and *N*-ethyl-*N*′-[(dimethylamino)-propyl]carbodiimide according to the manufacturer's instructions to permit covalent attachment of the applied peptides. Solutions of $AChE_{586-599}$, $BuChE_{573-586}$, and scrambled $AChE_{586-599}$ at 2 mg/mL in 0.1 M sodium acetate (pH 4.0) were applied to the chip, and one flow cell was left uncoated. The chip was then blocked with 1 M ethanolamine (pH 8.2) and washed with 0.1 M glycine (pH 2.6) to remove any unattached peptide. A 10 μg/mL solution of protein G-purified 105A diluted in HBS was applied to the chip, and the resulting sensorgrams were used for curve fitting with the BIAevaluation software. The analyte concentration is required to obtain the K_D and was estimated by measuring the protein concentration of the purified 105A by UV spectrophotometry at 220 and 340 nm and taking the molecular mass of IgG to be 150 kDa to produce a figure for the 105A concentration in the assay of 6 μM. Inaccuracy of this figure resulting from protein contaminants and inactive antibody would result in an underestimation of the affinity, since the effective analyte concentration would be lower than the figure that was obtained.

Detection of $AChE_{586-599}$ Oligomers Using a 105A Sandwich ELISA. For biotinylation of 105A, 20 μg of EZ-Link TFP-PEO-Biotin (Pierce) in 20 μL of *N*,*N*-dimethylformamide was added to 2 mg of protein G-purified 105A in 1 mL of PBS and incubated at room temperature for 1 h, after which unconjugated biotin was removed using a Microcon YM30 column (Millipore).

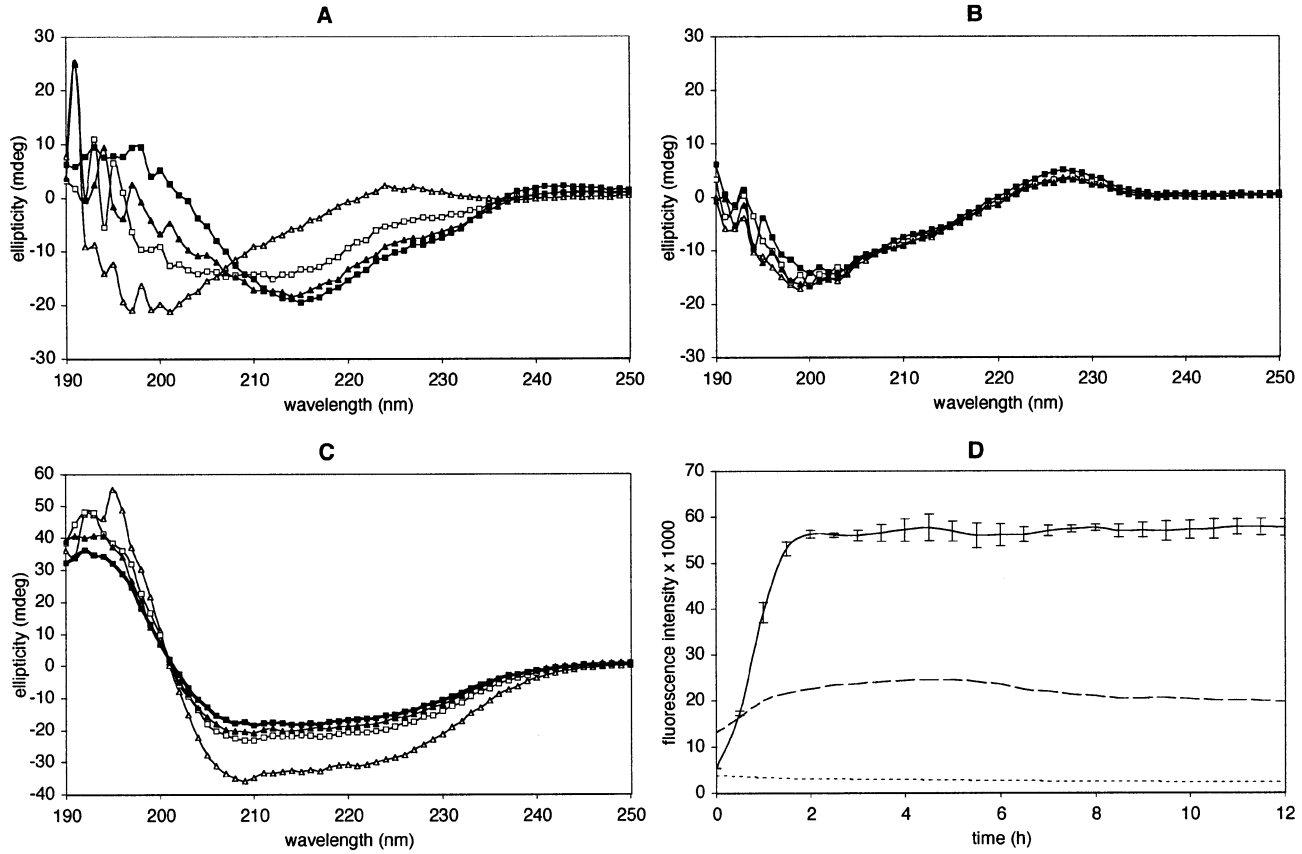

FIGURE 1: $AChE_{586-599}$, but neither $BuChE_{573-586}$ nor T_{40}, forms amyloid fibrils. Circular dichroism (CD) spectra of 200 μM $AChE_{586-599}$ (A), $BuChE_{573-586}$ (B), and T_{40} (C) peptide solutions taken 1 min (△), 90 min (□), 3 h (▲), and 18 h (■) after pH neutralization (to 7.0) of the aqueous peptide solutions (which are acidic, pH ≈4; see the text). Rapid amyloid fibril formation by $AChE_{586-599}$ is initiated, and the spectra record a shift in its conformation from random coil to β-sheet secondary structure. $BuChE_{573-586}$ displays no such shift in secondary structure. The T_{40} peptide has an α-helical secondary structure and does not exhibit a conformational shift; although there is a diminution of the signal intensity of the spectrum over time due to insolubility at neutral pH, the positions of the spectral maximum and minima remain constant. (D) Fluorescence of the hydrophobic dye ANS in 200 μM solutions of $AChE_{586-599}$ (—), T_{40} (- - -), and $BuChE_{573-586}$ (•••) immediately after neutralization, as above, monitored over time. $BuChE_{573-586}$ is unable to influence ANS fluorescence, but $AChE_{586-599}$ rapidly forms amyloid assemblies into which the hydrophobic dye is able to partition, with a concomitant increase in fluorescence (*66*−*68*). T_{40} does not form amyloid, but is able to recruit ANS into α-helix-rich structures. The error bars for the $BuChE_{573-586}$ and T_{40} data (representing the standard error of the mean value of duplicate samples) are too small to be depicted here ($<0.7 \times 10^3$).

Costar EIA/RIA plates were coated with 1 μg of protein G-purified 105A per well and blocked as for AChE immunoprecipitation (see above). Subsequent incubation steps (1 h duration) were performed using 100 μL volumes and were separated by three washes with 250 μL of PBS-Tween per well. $AChE_{586-599}$ solutions, freshly prepared by mixing equal volumes of aqueous peptide solutions and 2× PBS-Tween, were applied to the plate, allowing simultaneous oligomer formation and capture. The wells received 150 ng of biotinylated 105A per well to detect any captured oligomers. The biotin label was detected with 300 ng of streptavidin−peroxidase polymer (Sigma) per well and quantified with OPD substrate by measurement of the absorbance at 485 nm.

RESULTS

Biophysical Properties of $AChE_{586-599}$, $BuChE_{573-586}$, and T_{40}. The peptide $AChE_{586-599}$ has previously (*2*) been shown to form classical amyloid fibrils, consisting of 7 nm fibers which have a β-sheet-rich secondary structure and which bind thioflavin-T and Congo red (*22*). To investigate the effect of sequence upon $AChE_{586-599}$ fibrillogenesis, the biophysical properties of the related synthetic peptides $BuChE_{573-586}$ and T_{40} were compared to those of $AChE_{586-599}$ in a kinetic circular dichroism (CD) experiment (Figure 1A−C). Fibril assembly is initiated by the neutralization of aqueous solutions of $AChE_{586-599}$, which begin with a low pH (≈4 at 1 mM) due to residual trifluoroacetic acid from the peptide synthesis (*2*). A transition in $AChE_{586-599}$ conformation from random coil to β-sheet, associated with the formation of amyloid-type fibrils, occurs over a period of hours after pH neutralization (Figure 1A). Under the same experimental conditions, however, $BuChE_{573-586}$ does not exhibit such a conformational shift, but remains unstructured (Figure 1B). The solution remains nonturbid, and the peptide does not acquire thioflavin-T or Congo red binding capability (data not shown). $BuChE_{573-586}$ is not therefore capable of self-assembing into amyloid fibrils under conditions highly favorable for $AChE_{586-599}$ self-assembly. The T_{40} peptide, which encompasses the sequence of $AChE_{586-599}$, also does not form fibrils under the same experimental conditions. Rather than remaining unstructured, like $BuChE_{573-586}$, it displays a pH-independent α-helical conformation (Figure 1C), as has been predicted for the T-peptide domain of the parent enzyme (*13*). The stability of this conformation is indicated by the absence of any shift in the positions of the maximum and minima of the CD spectra. There is, however,

a diminution of the signal intensity in the CD spectra after 90 min, which can be attributed to rapid peptide precipitation (complete in <90 min) after neutralization. These α-helical T_{40} aggregates are amorphous (i.e., nonfibrillar), and they do not bind Congo red or thioflavin-T (data not shown).

The fluorescent dye 8-anilinonaphthalenesulfonic acid (ANS) can be used to probe hydrophobic environments formed by polypeptide chains (*66*−*68*). ANS fluorescence in the presence of $AChE_{586-599}$, $BuChE_{573-586}$, and T_{40} was monitored over a 12 h period immediately after neutralization, as for the CD experiments (Figure 1D). $AChE_{586-599}$ immediately begins to generate a hydrophobic environment permissive for ANS incorporation in the period preceding growth of fibrils and detection of a conformational change by CD. Conversely, $BuChE_{573-586}$ has no capacity to alter ANS fluorescence, consistent with its inability to form amyloid, and suggesting an insufficiency of a hydrophobic driving force for self-assembly. In the case of T_{40}, an increase in ANS fluorescence is detected, although both the rate and final level are lower than in the case of $AChE_{586-599}$. Since T_{40} remains α-helical (Figure 1C), the hydrophobic environment identified by the appearance of ANS fluorescence is likely to be the result of interactions between these structures (rather than stacked *β*-sheets in an amyloid fibril). The role of the amphiphilic T-peptide domain in AChE is to make homomeric contacts required for the tetramerization of the enzyme, a phenomenon which may also underlie the tendency of synthetic T_{40} to aggregate and bind ANS.

Conformation-Specific Immunoreagents for $AChE_{586-599}$, $BuChE_{573-586}$, and T_{40}. To investigate the structures adopted by the synthetic peptides and the T-peptide domain of AChE in situations that cannot be addressed spectroscopically, we generated two conformation-specific mouse monoclonal antibodies: 55C, produced by immunization with T_{40}, and 105A, produced by immunization with $AChE_{586-599}$. Figure 2A shows analysis of the specificity of the antibodies by an ELISA against synthetic peptide antigens. 105A reacts with the immunogen peptide $AChE_{586-599}$, but also displays a weaker cross-reactivity with $BuChE_{573-586}$. It reacts neither with a scrambled version of $AChE_{586-599}$ nor with any of three A*β* fragments, despite the sequence similarity between $AChE_{586-599}$ and A*β*. Furthermore, it does not react with T_{40}, even though the $AChE_{586-599}$ sequence is present within the longer peptide. The shorter $AChE_{586-599}$ peptide adopts either an unstructured or *β*-sheet conformation in CD experiments, but T_{40} has an α-helical conformation; therefore, 105A requires an extended or linear organization of the region of residues 586−599, which is not adopted by the sequence when resident within T_{40}.

A comparison of the reactivity of 55C in different experimental systems reveals that antibody recognition is dependent upon the native α-helical conformation of the antigen. While 55C labels T_{40} in ELISA and BIAcore experiments, in which the conformation of the antigen is not expected to be disrupted, it is incapable of labeling either T_{40} or T-peptide-containing AChE on denaturing Western blots (Figure 2C). This difference is not merely the result of attachment of the antigens to nitrocellulose, since 55C can detect both antigens on nondenaturing dot blots. The serum from the immunized mouse used to generate 55C is able to label both denatured and natively folded antigen (Figure 2C), revealing that 55C is a member of a subset of T_{40}-reactive

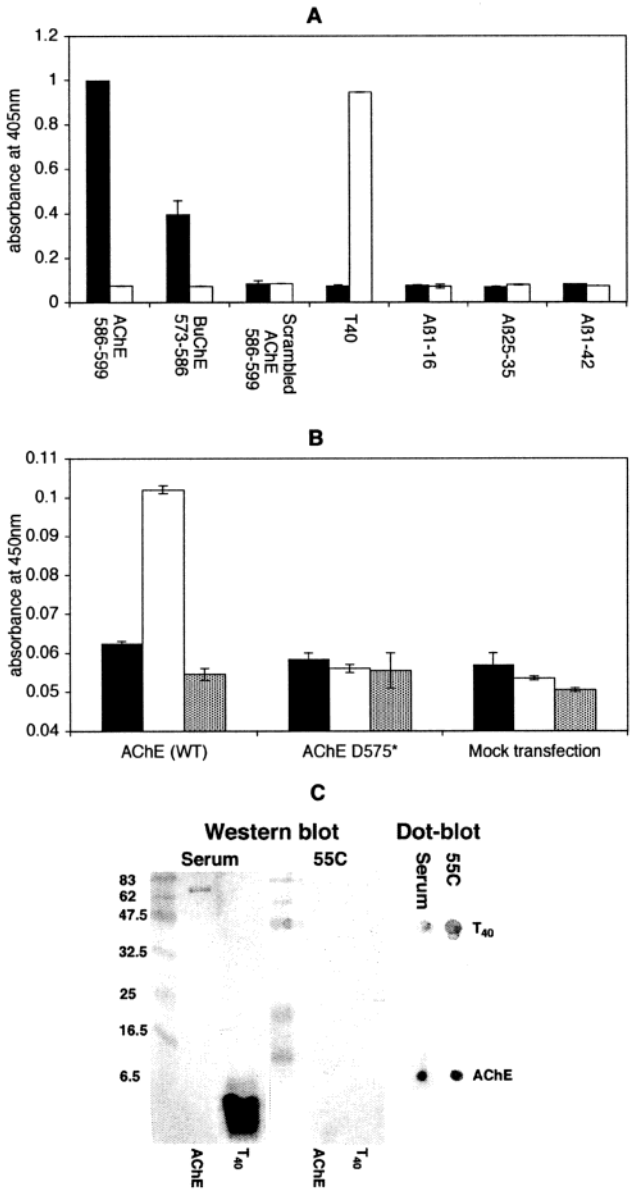

FIGURE 2: Monoclonal antibodies against $AChE_{586-599}$, $BuChE_{573-586}$, and T_{40}. (A) ELISA employing multiple synthetic peptide antigens probed with mouse monoclonal antibodies 105A (black) and 55C (white). 105A was raised against $AChE_{586-599}$, cross-reacts with $BuChE_{573-586}$, but does not label any of the other peptides, including T_{40}. 55C was raised against T_{40} and specifically labels only that peptide. (B) Immunoprecipitation of wild-type T-form human AChE (WT) and truncated AChE lacking the T-peptide (AChE D575*) by monoclonal antibodies 105A (black) and 55C (white) and an isotype-matched negative control antibody (gray) from conditioned culture medium. Human recombinant AChE was expressed in transiently transfected HEK293 cells, and a mock transfection serves as a negative control. (C) Western blot (left) and dot blot (right) of purified human recombinant wild-type AChE (∼65 kDa) and T_{40} (∼4 kDa) labeled with 55C and serum from the animal used to produce 55C. Both the parent serum and the monoclonal serum are capable of recognizing the antigens under native conditions on the dot blot, but only the parent serum and not 55C is able to label the same antigens on the Western blot of a denaturing SDS−PAGE gel.

immunoglobulins in the parent mouse that binds a conformation-dependent epitope. Consistent with the results of these experiments, 55C is able to immunoprecipitate wild-type (WT) T-form AChE from the conditioned culture medium of HEK293 cells expressing the recombinant enzyme (Figure

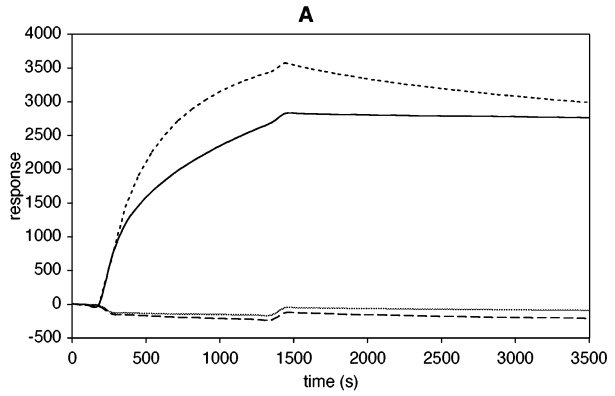

	k_a (1/ms)	k_d (1/s)	K_D (M)
105A-AChE$_{586-599}$	1.54E+04	5.08E-05	3.15E-09
105A-BuChE$_{573-586}$	6.17E+03	3.95E-04	6.40E-09

FIGURE 3: 105A has a similar affinity for AChE$_{586-599}$ and BuChE$_{573-586}$. (A) BIAcore sensorgrams obtained during flow of purified 105A through surface plasmon resonance sensor chip flow cells covalently coated with AChE$_{586-599}$ (—), BuChE$_{573-586}$ (- - -), and scrambled AChE$_{586-599}$ (— — —) and through an uncoated flow cell (···). A mass response that can be attributed to the binding of the antibody to the surface of the peptide-coated chip is seen in the case of AChE$_{586-599}$ and BuChE$_{573-586}$, but not in that of the scrambled peptide or the uncoated chip. (B) Kinetic parameters calculated by curve fitting software using the data shown in panel A. The affinity of 105A for BuChE$_{573-586}$ is approximately 2-fold lower than its affinity for AChE$_{586-599}$ (~7 vs ~3 nM), due mainly to the difference in the off-rate (k_d).

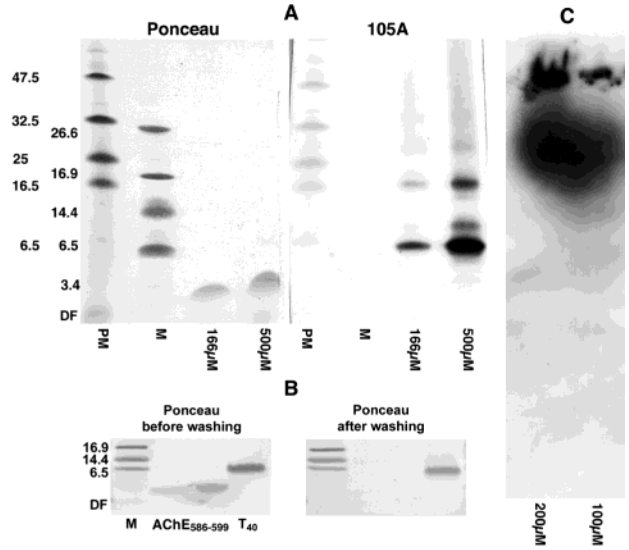

FIGURE 4: 105A labels AChE$_{586-599}$ fibrils and identifies an oligomeric species. (A) Western blots of denaturing SDS−PAGE gels loaded with AChE$_{586-599}$ at two concentrations (10 μL per lane) with prestained (PM) and nonprestained (M) markers, treated with Ponceau-S to stain for protein (left), and immunolabeled with 105A (right). 105A labels a series of higher-molecular mass bands, corresponding to SDS-resistant oligomers of AChE$_{586-599}$, which are not detected by the protein stain. No labeling of BuChE$_{573-586}$ by 105A is seen on similar Western blots (not shown). DF denotes the position of the dye front. (B) Similar Western blots loaded with the same two concentrations of AChE$_{586-599}$ and with T_{40} (200 μM) stained with Ponceau-S immediately following transfer (left) and after extensive washing in PBS (right). The band corresponding to monomeric AChE$_{586-599}$ is not present after washing. DF denotes the position of the dye front. (C) Western blot of a native, nondenaturing gel (lacking SDS and the reducing agent) loaded with AChE$_{586-599}$ at two concentrations (10 μL/lane). The peptide has formed large fibrillar aggregates, which migrate only a short distance into the gel, or are retained in the well, and 105A has labeled both these species.

2B). The AChE$_{586-599}$- and BuChE$_{573-586}$-specific monoclonal antibody 105A did not immunoprecipitate significant amounts of AChE (WT) from the culture medium. A truncation mutant, D575*, lacking the T-peptide, and not therefore capable of assembly into dimers and tetramers, retains full enzymatic activity, but is not recognized by 55C, confirming the specificity of the antibody for the T-peptide. The AChE T-peptide and synthetic T_{40} therefore share the ability to present a conformation-dependent epitope for recognition by 55C, indicating that the α-helical conformation of the synthetic T_{40} peptide is mirrored in that of the sequence when present as the C-terminal domain of the parent enzyme.

105A Has Similar Affinity for AChE$_{586-599}$ and BuChE$_{573-586}$. The different biophysical properties of the 105A antigens AChE$_{586-599}$ and BuChE$_{573-586}$, described above, complicate the evaluation of the significance of signal intensity differences in immunoassays, where peptide conformation may be unknown. To clarify this issue, the affinity of the antibody for the two antigens was measured by surface plasmon resonance (BIAcore) using conditions (pH 4.0) for covalent antigen immobilization known to be incompatible with AChE$_{586-599}$ fibrillogenesis (*2*). Measurement during chip loading confirmed that equal amounts of the peptides were bonded to the matrix. Figure 3 shows that the affinity of 105A for AChE$_{586-599}$ ($K_d \approx 3$ nM) is very similar to its affinity for BuChE$_{573-586}$ ($K_d \approx 7$ nm). No significant mass response is detected in flow cells coated with scrambled AChE$_{586-599}$ (Figure 3A) or T_{40} (data not shown). The approximately 2-fold difference in affinity can be attributed mainly to a difference in the dissociation rate, as is frequently the case for antibody−antigen interactions (*69*). The results of 105A ELISAs using BuChE$_{573-586}$ and AChE$_{586-599}$ antigens (Figure 2A) agree well with those obtained under the more controlled BIAcore conditions, so the different biophysical and fibrillogenic properties of the two peptides are not a major factor influencing signals obtained in these ELISAs.

AChE$_{586-599}$ but Not BuChE$_{573-586}$ Forms Oligomeric Species. The results of Western blotting of AChE$_{586-599}$ and BuChE$_{574-587}$ with 105A are, unlike ELISAs, influenced by the differing biophysical characteristics of the antigens. In this experimental system, there is no immunolabeling of BuChE$_{573-586}$ (data not shown), seemingly in disagreement with the results described above. On Western blots, the majority of the AChE$_{586-599}$ peptide migrates, as expected, as a band corresponding to the monomeric peptide, at approximately 2 kDa, and this band can be stained with Ponceau-S. However, 105A is not detected at this position, and it instead labels a ladder of additional higher-molecular mass bands that are not detected by the Ponceau protein stain. The absence of 105A labeling at a position corresponding to monomeric AChE$_{586-599}$ is explained by poor attachment of the monomeric antigen to nitrocellulose. Extensive washing of the membrane with PBS removes the Ponceau-stainable monomeric AChE band (Figure 4B), but not the larger T_{40} peptide or the marker proteins. BuChE$_{574-587}$ is removed from nitrocellulose even more readily than AChE$_{586-599}$ (data not shown), but in this case, nothing

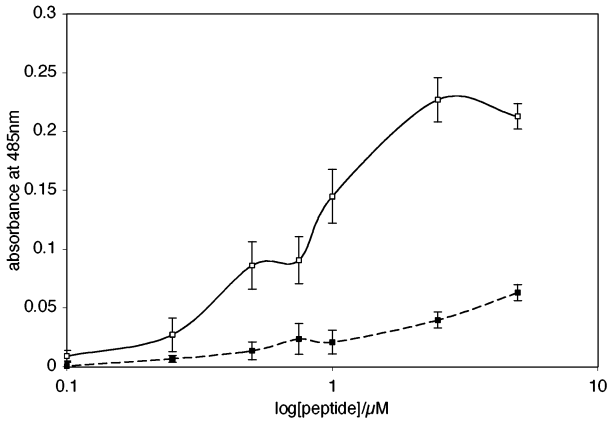

FIGURE 5: $AChE_{586-599}$ oligomers exist in solution. Single-antibody sandwich ELISA, employing purified unconjugated 105A to coat the plate, and biotinylated 105A to detect $AChE_{586-599}$ (—) or $BuChE_{573-586}$ (- - -) recruited by the immobilized antibody. This assay is designed to detect only multimeric species (see the text), and the signal obtained with $BuChE_{573-586}$ is negligible compared to that obtained with $AChE_{586-599}$.

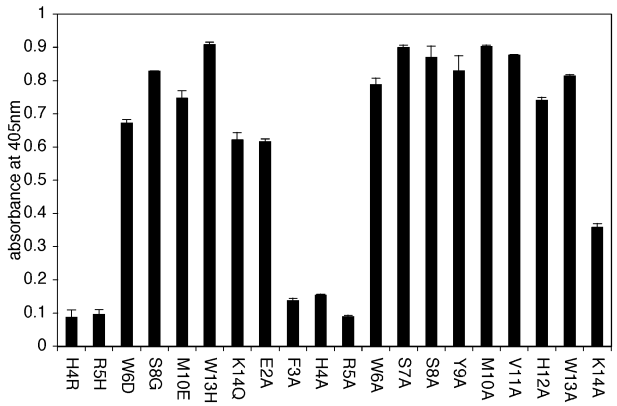

FIGURE 6: Epitope mapping of 105A. Mapping of the 105A epitope using mutant synthetic peptides in an ELISA. The mutations shown are replacements of individual residues with the cognate residue of Aβ (see Table 1) or with alanine. Residues 3−5 (FHR) are crucial for recognition by 105A; K14 exerts a smaller but significant effect.

remains for recognition by 105A. The amyloidogenic properties of $AChE_{586-599}$ result in the presence of a population of higher-molecular mass SDS-resistant oligomeric species of $AChE_{586-599}$ (but not of the nonamyloidogenic $BuChE_{573-586}$ peptide) that are available, unlike the monomeric molecule, for detection by 105A.

SDS-resistant oligomers of Aβ have been identified by protein staining of SDS−PAGE gels (*70*), but even the band corresponding to monomeric $AChE_{586-599}$ is near the limit of sensitivity of the conventional silver and Coomassie gel stains (data not shown), probably because of the small size of the polypeptide (14 amino acids). Omission of the reducing agent and the boiling step from the procedure does not affect the result (data not shown). The pH employed for SDS−PAGE is 6.8 in the stacking gel and 8.8 in the separating gel, both of which lie within the optimum pH window for $AChE_{586-599}$ self-assembly (*2*). The oligomeric species visible on 105A Western blots are therefore present in the low-pH starting solution, or are able to form rapidly at pH 6.8 in the presence of SDS.

In addition to small oligomers, gross amyloid aggregates and long fibrils are accessible to 105A, as shown by Western blotting of nondenaturing polyacrylamide gels lacking SDS (Figure 4C). The $AChE_{586-599}$ has in this case formed large aggregates of fibrils, most of which are unable to enter the gel at all, and remain in the well, but some of which are able to migrate a short distance into the matrix. The 105A epitope in $AChE_{586-599}$ is therefore exposed both on fibrils assembled into huge aggregates and on much smaller protofibrillar structures resistant to denaturation in SDS.To rule out the possibility that the oligomeric species seen on 105A-labeled Western blots are an artifact of the experimental conditions, a "sandwich"-type capture ELISA, able to detect $AChE_{586-599}$ oligomers under physiological conditions, was developed. The technique employs unconjugated 105A for capturing $AChE_{586-599}$ from solution, and biotinylated 105A for detecting any immobilized oligomers (Figure 5). $BuChE_{573-586}$ acts as an excellent negative control in this assay, because it does not form fibrils under conditions highly favorable for $AChE_{586-599}$ amyloidogenesis, and has been demonstrated by BIAcore to be a 105A antigen, as described above. Since the same monoclonal antibody is used for both capture and detection, the signal seen using $AChE_{586-599}$ in this system is the result of the presence of discrete species possessing more than one copy of the epitope. These species represent oligomeric or protofibrillar forms of the peptide, since the peptide concentrations used in the assay (<10 μM, with a detectable signal at 1 μM) are well below the published critical concentration (~50 μM) required for formation of classical, long amyloid fibrils by $AChE_{586-599}$ (*2*).

The 105A Epitope Lies Near the N-Terminus of $AChE_{586-599}$. The ability of 105A to label not only protofibrillar oligomers, both in solution and on Western blots, but also large aggregates of fibrils suggests that the epitope recognized by the antibody is exposed on the surface of both these structures. The 105A epitope was therefore mapped using a panel of mutant synthetic peptides as antigens in an ELISA. Single-point mutation of F3, H4, or R5, either to alanine or to the cognate residue from Aβ (H4R or R5H), is alone sufficient to abolish 105A immunoreactivity (Figure 5), but mutations C-terminal to this region do not affect the ability of the peptide to act as a 105A antigen. Results with nested truncation mutants (not shown) agree with the positioning of the epitope around Phe3−Arg5: removal of at least two N-terminal residues ablates 105A reactivity, and removal of up to seven C-terminal residues has no such effect. The 105A epitope, centered around FHR (positions 3−5), is therefore exposed on the surface of $AChE_{586-599}$ fibrils and protofibrillar oligomers, which can be recognized by the antibody in multiple experimental systems.

DISCUSSION

The C-terminal T-peptide domain of AChE (residues 575−614) is responsible for the assembly of the enzyme into homomeric soluble tetramers and heteromeric anchored tetramers to allow the enzyme to be positioned according to its functional role (*5*). We have used a combination of biophysical techniques and conformation-specific monoclonal antibodies to reveal the native conformation of the T-peptide and the structure of classical amyloid fibrils and protofibrils formed by a fragment of the T-peptide, $AChE_{586-599}$. A synthetic version of the T-peptide domain, T_{40}, forms an α-helix that is able to interact with itself and generate a

hydrophobic environment into which ANS partitions, consistent with the amphiphilic C-terminal domain being responsible for providing the adhesive force between disulfide-linked dimers in tetrameric AChE (*11*). We produced a conformation-specific monoclonal antibody, 55C, which has a requirement for the native α-helical conformation of its antigen. The ability of 55C to immunoreact not only with α-helical synthetic T_{40} but also with the natively folded T-peptide of full-length AChE reveals that the same, or a very similar, conformation is adopted by the sequence in the intact enzyme. To the best of our knowledge, this observation, while in perfect accord with the current understanding (*13*, *16*, *17*), is the first empirical evidence for an *in situ* α-helical conformation of the domain.

The native conformation of the T-peptide is disrupted in a shorter synthetic peptide, $AChE_{586-599}$, derived from a region of the sequence that is weakly homologous with the sequence of the Alzheimer's disease Aβ peptide (*1*, *2*). $AChE_{586-599}$ does not adopt the native α-helical conformation but, when buffered at physiological pH, rapidly forms classical β-sheet-rich fibrils which conform in every way to the "operational definition" (*22*) of amyloid, based on conformation, ultrastructure, and tinctorial properties. After it has been boiled in SDS, a fraction of $AChE_{586-599}$ is able to form resistant oligomeric species that can be detected by a second monoclonal antibody, 105A. The species are not sufficiently abundant to be detected by protein staining, and indeed, the majority of the peptide runs as a monomeric band, although, unlike the ladder of oligomeric species, it does not remain stably associated with nitrocellulose.

The critical concentration for formation of insoluble aggregates of $AChE_{586-599}$ fibrils has been previously reported to be 50 μM (*2*), a value similar to the published critical concentration (10−40 μM) for Aβ fibrillogenesis (*22*). Simple spectroscopical techniques are not sufficiently sensitive to detect soluble fibrillar or protofibrillar species, which may be formed only by a fraction of the available peptide below the critical concentration (for example, 200 μM $AChE_{586-599}$ is generally required for CD, Congo red, and thioflavin-T spectroscopy). We used a 105A sandwich ELISA to detect oligomeric species of $AChE_{586-599}$ at 100-fold lower concentrations ($\geq$0.5 μM) after an incubation time of only 1 h in physiological buffer. The presence of these species at concentrations well below the critical threshold for gross amyloid formation may explain the absence of a lag phase following initiation of $AChE_{586-599}$ fibrillization by neutralization of low-pH stocks (*2*). While the CD spectra of these solutions indicate that the majority of the peptide is unstructured and monomeric (as is also the case for Western-blotted material), they may contain small amounts of protofibrillar "seeds" capable of nucleating rapid fiber extension under permissive pH conditions.

Since 105A can label long fibrils assembled into aggregates, in which the peptide is known to have a β-sheet secondary structure, it is probable that the protofibrillar nuclei identified using 105A also possess a β-sheet secondary structure. Aβ oligomers have been detected using SDS−PAGE (*70*), size exclusion chromatography (*71*), atomic force microscopy (*72*, *73*), and Aβ-specific immunoreagents (*74*). The studies using 105A therefore confirm the identification of $AChE_{586-599}$ as a typical amyloidogenic peptide, capable of forming both long fibrils and smaller oligomeric species. It has been suggested that soluble protofibrils, rather than gross fibrillar aggregates, are the species responsible for exerting the toxic pathological effects of amyloidogenic polypeptides (*25*−*27*, *30*).

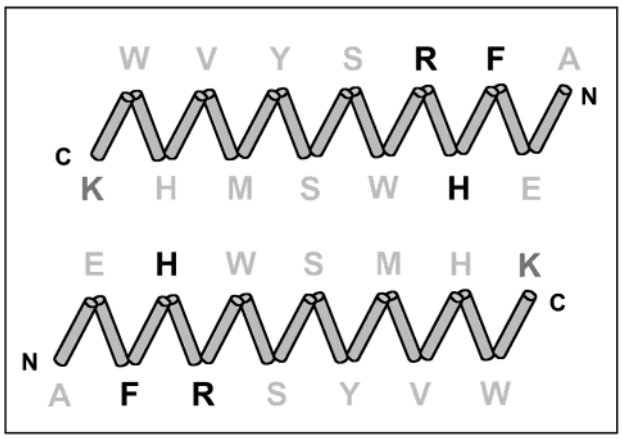

FIGURE 7: Model of antiparallel pairing of the $AChE_{586-599}$ β-sheet. Structure of $AChE_{586-599}$ fibrils and protofibrils suggested by a 105A capture ELISA (Figure 5) and epitope mapping (Figure 6). Black residues are critical for the 105A epitope and light gray residues unimportant, while K14, which is not required for but can affect antibody binding, has an intermediate coloring.

The mapping of the 105A epitope to FHR (residues 3−5 of $AChE_{586-599}$) implies that this region is exposed on the surface of fibrils and protofibrils. The oligomeric protofibrils identified by Western blotting are mostly $\leq$15 kDa, and it is hard to imagine how such small species would be able to interact simultaneously with two identical immunoglobulins in the sandwich ELISA if all the epitopes were to lie on one side of the assembly. An antiparallel β-sheet conformation for $AChE_{586-599}$ fibrils and protofibrils therefore seems likely (Figure 7). This model displays favorable hydrophobic interactions and salt bridges between charged residues E2 and K14. Further evidence for such a model is the observation that mutation of K14 to alanine has a modest negative effect on 105A recognition, though it is not as extensive as that of mutation of F3, H4, or R5, any of which is alone sufficient to completely ablate reactivity. An antiparallel arrangement allows residue 14 to lie adjacent to the epitope at FHR, where it might be able to exert direct or indirect effects upon antibody recognition. Interestingly, anti-Aβ antibodies with epitopes at the cognate position in Aβ (EFRH) are able to disrupt fibril formation by the peptide (*75*, *76*), suggesting that, if there is, as posited, a commonality of structure as well as sequence, the N-terminal region of both $AChE_{586-599}$ and Aβ (*77*, *78*) is likely to be a key determinant of higher-order structure.

A factor responsible for the amyloidogenic properties of $AChE_{586-599}$ is the apparent lack of drive toward the native α-helical conformation, presumably due to the absence of T-peptide sequence both upstream and downstream of the fragment. Such disruption of the native fold may be necessary, but is not sufficient for amyloidogenesis, since $BuChE_{573-586}$, the cognate peptide from the closely related enzyme butyrylcholinesterase, has a random coil conformation both before and after neutralization, but was not found to form β-sheet-rich fibrils or 105A-detectable protofibrils in the experiments described herein. We have not, however, addressed the question of whether $BuChE_{573-586}$ fiber growth

can be induced, for example, by application of exogenous seeds consisting of preformed oligomeric or fibrillar $AChE_{586-599}$ (or perhaps even Aβ). The sequence differences between AChE and BuChE do not substantially reduce the hydrophobicity (which is likely to play an important role in driving fibril assembly), since the aromatic residues required for amphiphilic T-peptide-driven enzyme oligomerization are highly conserved (*79*). Deprotonation of the two $AChE_{586-599}$ histidine residues as the pH is brought to neutral is crucial for fibrillogenesis (*2*), so the substitution of H12 with a negatively charged aspartate in $BuChE_{573-586}$ may play a role in reducing the tendency of the latter peptide to form fibrils. The loss of the negative charge at E2 might also be important, if the residue is involved in formation of a salt bridge. Both of these considerations are in agreement with the antiparallel model (Figure 7), which predicts juxtaposition both of the histidines and of E2 and K14. Furthermore, both E2 and H12 are present in $AChE_{586-599}$ and Aβ, but not in $BuChE_{573-586}$.

Diverse polypeptides, including those not implicated in disease, can be induced in the laboratory to form amyloid fibrils possessing the generic β-sheet structure (*37*−*42*). Nevertheless, under a given set of conditions (the most interesting and important of which, it could be argued, are physiological), sequence is, perhaps not unexpectedly, critically important to the ability of a peptide to spontaneously form amyloid fibrils. We have not addressed in this paper the possibility that AChE *in vivo* can contain, or give rise to fragments containing, the aberrant β-sheet structure that we have characterized *in vitro*. The use of the conformation-specific antibodies 55C and 105A to probe structural changes in the T-peptide of AChE both *in vitro* and *ex vivo* may provide insight into these possibilities.

ACKNOWLEDGMENT

We thank the Oxford Centre for Molecular Science for access to CD and peptide synthesis facilities. We are grateful to Mr. M. Coates and Dr. G. MacPherson of the Sir William Dunn School of Pathology for performing immunizations, and to Mr. T. Dwyer of Synaptica Ltd. for technical assistance with the sandwich ELISA.

REFERENCES

1. Greenfield, S. A., and Vaux, D. J. (2002) *Neuroscience 113*, 485−492.
2. Cottingham, M. G., Hollinshead, M. S., and Vaux, D. J. (2002) *Biochemistry 41*, 13539−13547.
3. Silver, A. (1974) *The Biology of Cholinesterases*, North-Holland, Amsterdam.
4. Massoulie, J. (2002) *Neurosignals 11*, 130−143.
5. Massoulie, J., Anselmet, A., Bon, S., Krejci, E., Legay, C., Morel, N., and Simon, S. (1999) *Chem.-Biol. Interact. 119*−*120*, 29−42.
6. Bon, S., Coussen, F., and Massoulie, J. (1997) *J. Biol. Chem. 272*, 3016−3021.
7. Perrier, A. L., Massoulie, J., and Krejci, E. (2002) *Neuron 33*, 275−285.
8. Sussman, J. L., Harel, M., Frolow, F., Oefner, C., Goldman, A., Toker, L., and Silman, I. (1991) *Science 253*, 872−879.
9. Bourne, Y., Taylor, P., Bougis, P. E., and Marchot, P. (1999) *J. Biol. Chem. 274*, 2963−2970.
10. Bourne, Y., Grassi, J., Bougis, P. E., and Marchot, P. (1999) *J. Biol. Chem. 274*, 30370−30376.
11. Blong, R. M., Bedows, E., and Lockridge, O. (1997) *Biochem. J. 327*, 747−757.
12. Simon, S., Krejci, E., and Massoulié, J. (1998) *EMBO J. 17*, 6178−6187.
13. Giles, K. (1997) *Protein Eng. 10*, 677−685.
14. Morel, N., Leroy, J., Ayon, A., Massoulie, J., and Bon, S. (2001) *J. Biol. Chem. 276*, 37379−37389.
15. Velan, B., Grosfeld, H., Kronman, C., Leitner, M., Gozes, Y., Lazar, A., Flashner, Y., Marcus, D., Cohen, S., and Shafferman, A. (1991) *J. Biol. Chem. 266*, 23977−23984.
16. Massoulie, J., Pezzementi, L., Bon, S., Krejci, E., and Vallette, F. M. (1993) *Prog. Neurobiol. 41*, 31−91.
17. Harel, M., Dvir, H., Bon, S., Liu, W. Q., Garbay, C., Sussman, J. L., Massoulié, J., and Silman, I. (2002) The VIIth International Meeting on Cholinesterases, Pucòn, Chile (poster).
18. Harel, M., Dvir, H., Bon, S., Liu, W. Q., Garbay, C., Sussman, J. L., Massoulie, J., and Silman, I. (2002) in *XIth International Symposium on Cholinergic Mechanisms: Function and Dysfunction* (Soreq, H., and Fisher, A., Eds.) Martin Dunitz, London.
19. Glenner, G. G., and Wong, C. W. (1984) *Biochem. Biophys. Res. Commun. 120*, 885−890.
20. Kang, J., Lemaire, H. G., Unterbeck, A., Salbaum, J. M., Masters, C. L., Grzeschik, K. H., Multhaup, G., Beyreuther, K., and Muller-Hill, B. (1987) *Nature 325*, 733−736.
21. Selkoe, D. J., and Hardy, J. (2002) *Science 297*, 353−356.
22. Harper, J. D., and Lansbury, P. T., Jr. (1997) *Annu. Rev. Biochem. 66*, 385−407.
23. McLean, C. A., Cherny, R. A., Fraser, F. W., Fuller, S. J., Smith, M. J., Beyreuther, K., Bush, A. I., and Masters, C. L. (1999) *Ann. Neurol. 46*, 860−866.
24. Lambert, M. P., Barlow, A. K., Chromy, B. A., Edwards, C., Freed, R., Liosatos, M., Morgan, T. E., Rozovsky, I., Trommer, B., Viola, K. L., Wals, P., Zhang, C., Finch, C. E., Krafft, G. A., and Klein, W. L. (1998) *Proc. Natl. Acad. Sci. U.S.A. 95*, 6448−6453.
25. Walsh, D. M., Hartley, D. M., Kusumoto, Y., Fezoui, Y., Condron, M. M., Lomakin, A., Benedek, G. B., Selkoe, D. J., and Teplow, D. B. (1999) *J. Biol. Chem. 274*, 25945−25952.
26. Walsh, D. M., Klyubin, I., Fadeeva, J. V., Cullen, W. K., Anwyl, R., Wolfe, M. S., Rowan, M. J., and Selkoe, D. J. (2002) *Nature 416*, 535−539.
27. Dahlgren, K. N., Manelli, A. M., Blaine Stine, W. J., Baker, L. K., Krafft, G. A., and LaDu, M. J. (2002) *J. Biol. Chem. 277*, 32046−32053.
28. Ward, R. V., Jennings, K. H., Jepras, R., Neville, W., Owen, D. E., Hawkins, J., Christie, G., Davis, J. B., George, A., Karran, E. H., and Howlett, D. R. (2000) *Biochem. J. 348*, 137−144.
29. Lue, L.-F., Kuo, Y.-M., Roher, A. E., Brachova, L., Shen, Y., Sue, L., Beach, T., Kurth, J. H., Rydel, R. E., and Rogers, J. (1999) *Am. J. Pathol. 155*, 853−862.
30. Sponne, I., Fifre, A., Drouet, B., Klein, C., Koziel, V., Pincon-Raymond, M., Olivier, J.-L., Chambaz, J., and Pillot, T. (2002) *J. Biol. Chem.* (in press).
31. Kayed, R., Head, E., Thompson, J. L., McIntire, T. M., Milton, S. C., Cotman, C. W., and Glabe, C. G. (2003) *Science 300*, 486−489.
32. Kisilevsky, R., and Fraser, P. E. (1997) *Crit. Rev. Biochem. Mol. Biol. 32*, 361−404.
33. Rochet, J. C., and Lansbury, P. T., Jr. (2000) *Curr. Opin. Struct. Biol. 10*, 60−68.
34. Sunde, M., Serpell, L. C., Bartlam, M., Fraser, P. E., Pepys, M. B., and Blake, C. C. (1997) *J. Mol. Biol. 273*, 729−739.
35. Dobson, C. M. (1999) *Trends Biochem. Sci. 24*, 329−332.
36. Lansbury, P. T., Jr. (1999) *Proc. Natl. Acad. Sci. U.S.A. 96*, 3342−3344.
37. Bucciantini, M., Giannoni, E., Chiti, F., Baroni, F., Formigli, L., Zurdo, J., Taddei, N., Ramponi, G., Dobson, C. M., and Stefani, M. (2002) *Nature 416*, 507−511.
38. Chiti, F., Webster, P., Taddei, N., Clark, A., Stefani, M., Ramponi, G., and Dobson, C. M. (1999) *Proc. Natl. Acad. Sci. U.S.A. 96*, 3590−3594.
39. Fandrich, M., Fletcher, M. A., and Dobson, C. M. (2001) *Nature 410*, 165−166.
40. Gross, M., Wilkins, D. K., Pitkeathly, M. C., Chung, E. W., Higham, C., Clark, A., and Dobson, C. M. (1999) *Protein Sci. 8*, 1350−1357.
41. Jimenez, J. L., Guijarro, J. I., Orlova, E., Zurdo, J., Dobson, C. M., Sunde, M., and Saibil, H. M. (1999) *EMBO J. 18*, 815−821.
42. Pertinhez, T. A., Bouchard, M., Tomlinson, E. J., Wain, R., Ferguson, S. J., Dobson, C. M., and Smith, L. J. (2001) *FEBS Lett. 495*, 184−186.
43. Kasa, P., Rakonczay, Z., and Gulya, K. (1997) *Prog. Neurobiol. 52*, 511−535.

44. Arendt, T., Bruckner, M. K., Lange, M., and Bigl, V. (1992) *Neurochem. Int. 21*, 381−396.
45. Geula, C., Mesulam, M. M., Saroff, D. M., and Wu, C. K. (1998) *J. Neuropathol. Exp. Neurol. 57*, 63−75.
46. Mesulam, M. M., and Geula, C. (1990) *Adv. Neurol. 51*, 235−240.
47. Smith, A. D., and Cuello, A. C. (1984) *Lancet 1*, 513.
48. Schegg, K. M., Harrington, L. S., Neilsen, S., Zweig, R. M., and Peacock, J. H. (1992) *Neurobiol. Aging 13*, 697−704.
49. Atack, J. R., Perry, E. K., Bonham, J. R., Perry, R. H., Tomlinson, B. E., Blessed, G., and Fairbairn, A. (1983) *Neurosci. Lett. 40*, 199−204.
50. Younkin, S. G., Goodridge, B., Katz, J., Lockett, G., Nafziger, D., Usiak, M. F., and Younkin, L. H. (1986) *Fed. Proc. 45*, 2982−2988.
51. Wright, C. I., Geula, C., and Mesulam, M. M. (1993) *Ann. Neurol. 34*, 373−384.
52. Geula, C., Greenberg, B. D., and Mesulam, M. M. (1994) *Brain Res. 644*, 327−330.
53. Moran, M. A., Mufson, E. J., and Gomez-Ramos, P. (1993) *Acta Neuropathol. 85*, 362−369.
54. Gomez-Ramos, P., Mufson, E. J., and Moran, M. A. (1992) *Brain Res. 569*, 229−237.
55. Ulrich, J., Meier-Ruge, W., Probst, A., Meier, E., and Ipsen, S. (1990) *Acta Neuropathol. 80*, 624−628.
56. Carson, K. A., Geula, C., and Mesulam, M. M. (1991) *Brain Res. 540*, 204−208.
57. Inestrosa, N. C., and Alarcon, R. (1998) *J. Physiol. 92*, 341−344.
58. Inestrosa, N. C., Alvarez, A., Perez, C. A., Moreno, R. D., Vicente, M., Linker, C., Casanueva, O. I., Soto, C., and Garrido, J. (1996) *Neuron 16*, 881−891.
59. Alvarez, A., Alarcon, R., Opazo, C., Campos, E. O., Munoz, F. J., Calderon, F. H., Dajas, F., Gentry, M. K., Doctor, B. P., De Mello, F. G., and Inestrosa, N. C. (1998) *J. Neurosci. 18*, 3213−3223.
60. Alvarez, A., Opazo, C., Alarcon, R., Garrido, J., and Inestrosa, N. C. (1997) *J. Mol. Biol. 272*, 348−361.
61. Laemmli, U. K., Beguin, F., and Gujer-Kellenberger, G. (1970) *J. Mol. Biol. 47*, 69−85.
62. Boussif, O., Lezoualc'h, F., Zanta, M. A., Mergny, M. D., Scherman, D., Demeneix, B., and Behr, J. P. (1995) *Proc. Natl. Acad. Sci. U.S.A. 92*, 7297−7301.
63. Kronman, C., Velan, B., Gozes, Y., Leitner, M., Flashner, Y., Lazar, A., Marcus, D., Sery, T., Papier, Y., Grosfeld, H., et al. (1992) *Gene 121*, 295−304.
64. Ellman, G. L., Courtney, K. O., Andrres, V., and Featherstone, R. M. (1961) *Biochem. Pharmacol. 7*, 88−95.
65. Karnovsky, M. J., and Roots, L. (1964) *J. Histochem. Cytochem. 12*, 219−221.
66. Kremer, J. J., Pallitto, M. M., Sklansky, D. J., and Murphy, R. M. (2000) *Biochemistry 39*, 10309−10318.
67. Lashuel, H. A., Wurth, C., Woo, L., and Kelly, J. W. (1999) *Biochemistry 38*, 13560−13573.
68. McParland, V. J., Kad, N. M., Kalverda, A. P., Brown, A., Kirwin-Jones, P., Hunter, M. G., Sunde, M., and Radford, S. E. (2000) *Biochemistry 39*, 8735−8746.
69. Mason, D. W., and Williams, A. F. (1986) in *Handbook of Experimental Immunology* (Weir, D. M., Ed.) p 38.1, Blackwell, Oxford, U.K.
70. Soreghan, B., Kosmoski, J., and Glabe, C. (1994) *J. Biol. Chem. 269*, 28551−28554.
71. Walsh, D. M., Lomakin, A., Benedek, G. B., Condron, M. M., and Teplow, D. B. (1997) *J. Biol. Chem. 272*, 22364−22372.
72. Harper, J. D., Lieber, C. M., and Lansbury, P. T., Jr. (1997) *Chem. Biol. 4*, 951−959.
73. Harper, J. D., Wong, S. S., Lieber, C. M., and Lansbury, P. T. (1997) *Chem. Biol. 4*, 119−125.
74. El-Agnaf, O. M., Mahil, D. S., Patel, B. P., and Austen, B. M. (2000) *Biochem. Biophys. Res. Commun. 273*, 1003−1007.
75. Frenkel, D., Balass, M., Katchalski-Katzir, E., and Solomon, B. (1999) *J. Neuroimmunol. 95*, 136−142.
76. Frenkel, D., Balass, M., and Solomon, B. (1998) *J. Neuroimmunol. 88*, 85−90.
77. Soto, C., Castano, E. M., Frangione, B., and Inestrosa, N. C. (1995) *J. Biol. Chem. 270*, 3063−3067.
78. Szendrei, G. I., Prammer, K. V., Vasko, M., Lee, V. M., and Otvos, L., Jr. (1996) *Int. J. Pept. Protein Res. 47*, 289−296.
79. Altamirano, C. V., and Lockridge, O. (1999) *Chem.-Biol. Interact. 119−120*, 53−60.

BI034768I